

ANALYTICAL AND NUMERICAL CALCULATIONS OF BEAM PIPE IMPEDANCES AT LOW FREQUENCIES WITH APPLICATION TO THIN SIS100 PIPE

U. Niedermayer*, O. Boine-Frankenheim and L. Hänichen

Technische Universität Darmstadt, Institut für Theorie Elektromagnetischer Felder,
Schlossgartenstrae 8, 64289 Darmstadt, Germany

Abstract

The projected fast ramped synchrotron SIS100 for FAIR uses an elliptical stainless steel beam pipe of 0.3 mm thickness. The lowest coherent betatron sidebands reach down to 100 kHz which demands accurate impedance calculations in the low frequency (LF) regime. For these frequencies, i.e. skin depth greater than wall thickness, structures behind the pipe may contribute to the impedance. Due to the extremely large wake length numerical methods in the time domain are not applicable. The longitudinal and transverse impedance of the thin SIS100 beam pipe including structures behind the pipe are obtained numerically by a method using power loss in the frequency domain. We compare different analytical models for simplified pipe structures to the numerical results. The dc and ultra-relativistic limits are investigated. The interpretation of bench measurements in the LF regime is discussed.

FORMULATION OF THE PROBLEM

This work is dedicated to the resistive wall coupling impedance of the SIS100 beampipe shown in Fig. 1. Since the imaginary part of the coupling impedance is dominated by space charge effects, the problem reduces to the determination of the real part of the coupling impedance. The real part of coupling impedance describes the resistive power loss of the beam that is responsible for wall heating and instability growth.

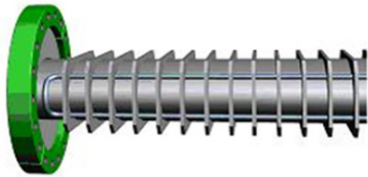


Figure 1: Proposed SIS100 pipe

The beam in a synchrotron is modeled as a disc of surface charge density σ traveling with velocity v . The displacement d_x of the beam (i.e. a coherent dipole oscillation) can be approximated to first order by

$$\sigma(\varrho, \varphi) \approx \frac{q}{\pi a^2} (\Theta(a - \varrho) + \delta(a - \varrho) d_x \cos \varphi). \quad (1)$$

The force acting back on the beam is described by the coupling impedance [1]

$$\underline{Z}_{\parallel}(\omega) = -\frac{1}{q^2} \int_{beam} \vec{E} \cdot \vec{J}_{\parallel}^* dV \quad (2)$$

$$\underline{Z}_{\perp,x}(\omega) = -\frac{v}{(qd_x)^2 \omega} \int_{beam} \vec{E} \cdot \vec{J}_{\perp}^* dV. \quad (3)$$

These expressions represent the beam's power loss divided by its current squared. The beam current in frequency domain (FD) is obtained from Eq. 1 as

$$\underline{J}_{s,z}(\varrho, \varphi, z; \omega) = \underline{J}_{\parallel} + \underline{J}_{\perp} = \sigma(\varrho, \varphi) e^{-i\omega z/v} \quad (4)$$

such that its magnitude is independent of the beam velocity. This leads to a magnetic field in FD that is also independent of v and therefore, the transverse resistive wall impedance obtained by Eq. 3 is linear in v . The charge density corresponding to Eq. 4 is

$$\underline{\rho}_s(\varrho, \varphi, z; \omega) = \frac{1}{v} \sigma(\varrho, \varphi) e^{-i\omega z/v} \quad (5)$$

which plays a major role for the longitudinal resistive wall impedance. In the following both the beam current and charge will be used as source terms in the Helmholtz equation.

AXIAL WAVES VERSUS RADIAL WAVES

In vacuum or metal, i.e. $\mu = \mu_0$ and $\varepsilon = \varepsilon_0$, the Helmholtz equation for the longitudinal electric field in frequency domain (FD) reads

$$\left(\Delta_{\perp} - i\omega\mu\kappa - \frac{\omega^2}{\beta^2\gamma^2 c^2} \right) \underline{E}_z = -\frac{i\omega\mu\sigma}{\beta^2\gamma^2} e^{-i\omega z/v} \quad (6)$$

where the r.h.s. represents both the source charge and current. This is a modified Bessel equation in cylindrical coordinates, i.e. the radial dependence is aperiodic. Since the complex exponential describes axial wave propagation this setup will be addressed as axial model [2]. If the setup of wire bench measurements is considered, it is possible to obtain radially propagating waves as well. For a short device under test, i.e. $l \ll \lambda$, the longitudinal phase advance is small and therefore one can approximate this setup by an entirely 2D model. This means $\partial_z = 0$ and subsequently the charge is static and the coupling impedance is only due to the current in the wire. The model equation becomes

$$(\Delta_{\perp} - i\omega\mu\kappa + \omega^2\mu\varepsilon) \underline{E}_z = i\omega\mu\sigma \quad (7)$$

* u.niedermayer@gmx.de

which is an ordinary Bessel equation describing radially propagating waves. Note that the axial model agrees with the radial one if $\beta \rightarrow \infty$ is applied [2]. Since infinite velocity is unphysical, the two models have to be distinguished properly.

Both Eqs. 6 and 7 have been solved for \underline{E}_z and subsequently for the coupling impedances using a formalized field matching technique. This has been implemented in Mathematica®[7] for an arbitrary number of concentric cylindrical layers which allows studies of characteristic frequencies and different boundary conditions.

Figures 2 and 3 show the wall current at unit beam current for a circular beampipe with radius $b = 40$ mm, thickness $d = 0.3$ mm and conductivity $\kappa = 1.4 \times 10^6$ S/m (in the following, these data will be used exemplary). The frequency ω_g with $|I_w(\omega_g)|/I_b = 1/\sqrt{2}$ (the onset of wall current) can be approximated employing lumped element circuits. For the monopolar case one obtains approximately

$$\omega_{g,\parallel} \approx \frac{R}{L_{pipe}} \approx \frac{1}{\mu\kappa b d \ln \frac{h_2}{b+d}} \quad (8)$$

whereas in the dipolar case one obtains ([3],[4])

$$\omega_{g,\perp} \approx \frac{R_{\perp}}{L_{\perp}} \approx \frac{2}{\mu\kappa b d}, \quad (9)$$

independent of the boundary radius h_2 . This important difference between monopole and higher multipoles follows from the location of the mutual flux inside the pipe.

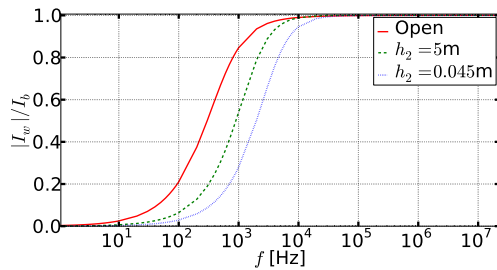


Figure 2: Monopolar wall current in the radial model with boundary radius h_2 as parameter

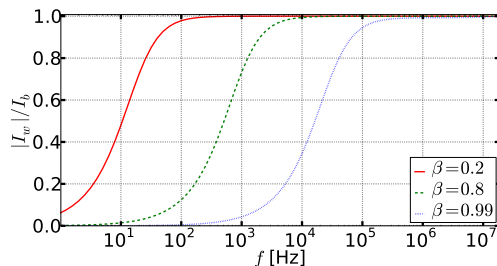


Figure 3: Monopolar wall current in the axial model with open boundary. For a closed boundary, similar dependencies as for the radial model are obtained.

Therefore and due to the independence of the magnetic field on the velocity (see Eq. 4), one expects agreement between both models for the transverse impedance result. In the ultrarelativistic case, the axial and the radial model disagree at the longitudinal impedance result. This is due to the surface impedance on the outside of the pipe which vanishes in the ultrarelativistic case ('pancake-field').

LF NUMERICAL MODEL

The radial model gives rise to a numerical method employing power loss to determine the resistive wall coupling impedance. The power loss can be determined via a post-processing template in e.g. CST EM-Studio®[6]. The connection to the real part of the impedance is [5]

$$\frac{\text{Re}\{Z_{\parallel}\}}{l} = \frac{1}{I^2} \frac{\delta P}{\delta z} = \frac{1}{I^2} \frac{1}{2} \int_{pipe} \underline{\vec{E}} \cdot \underline{\vec{J}}^* dV \quad (10)$$

$$\frac{\text{Re}\{Z_{\perp,x}(\omega)\}}{l} = \frac{c}{\omega d_x^2} \frac{1}{I^2} \frac{\delta P}{\delta z}. \quad (11)$$

Figures 4 and 5 show a comparison of the analytical ap-

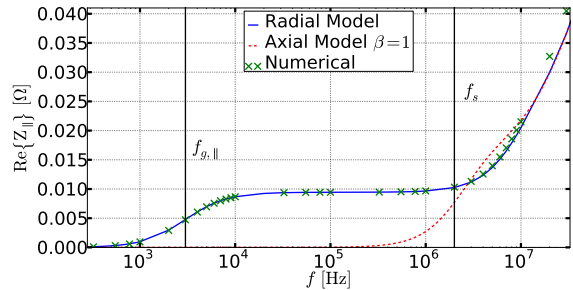


Figure 4: Comparison of analytical and numerical longitudinal impedance for a circular beampipe

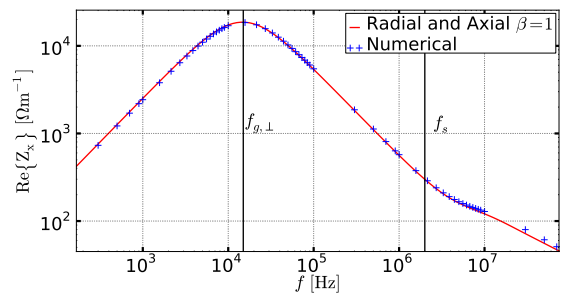


Figure 5: Comparison of analytical and numerical transverse impedance for a circular beampipe

proaches and a numerical calculation via Eqs. 10 and 11. The characteristic skin-effect frequency is given by $f_s = 1/(\pi\mu\kappa d^2) \approx 2$ MHz. The plateau for the longitudinal impedance is the Ohmic resistance $R \approx 10$ mΩ. The frequency on which the longitudinal impedance is half the

Ohmic resistance is given by $f_{g,\perp} = \omega_{g,\parallel}/2\pi \approx 3$ kHz at the onset of the wall current. This is also equivalent to the onset of the pipe's shielding property. Note that the value obtained by Eq. 8 corresponds only to the radial model.

The transverse impedance reaches a maximum at $f_{g,\perp} = \omega_{g,\perp}/2\pi \approx 15$ kHz which also represents the onset of the dipolar wall current and the onset of the shielding of dipolar beam oscillations.

PREDICTIONS FOR THE SIS100 BEAMPIPE

The SIS100 beampipe is supposed to serve as a cryo-adsorption pump which means that the temperature has to be kept below 10 K. In order to compensate the heat due to eddy currents during the magnet ramp, cooling tubes are considered to be attached on the outside of the beampipe. Figure 6 shows different proposed setups where the box around the pipe represents a worst case scenario of bad conducting material in the vicinity of the beampipe. Since the

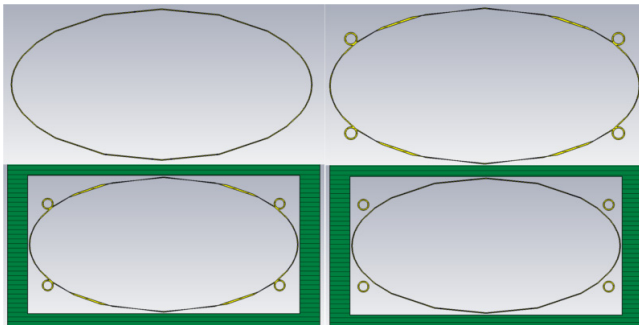


Figure 6: Proposed SIS100 beampipe setups

longitudinal impedance of the SIS100 pipe causes only a negligibly small heat load, it will not be discussed here.

The real part of the transverse impedance of the SIS100 pipe as it is relevant for coherent transverse instabilities has been obtained numerically. Figures 7 and 8 show that there is an influence on the outside equipment, as analytically expected, only below the frequency of onset of wall current. Above this frequency, the pipe shields well and therefore the impedance values for all setups coincide. Note that these results cannot be obtained by the analytic theory for circular pipes since an equivalent radius would become frequency dependent. Another important remark is that a significant resistive wall impedance increase is to be expected in case of closed orbit deviations.

CONCLUSION

The question if outside equipment contributes to the coupling impedance has been answered by a numerical analysis. A numerical method using power loss has been successfully validated for the transverse impedance and applied to the elliptical SIS100 pipe including outside equipment. Different results for the transverse impedance of dif-

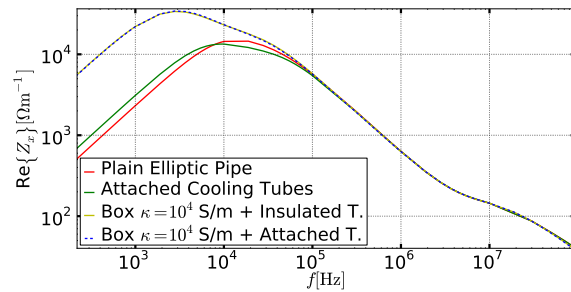


Figure 7: Horiz. imp. of proposed SIS100 pipe setups

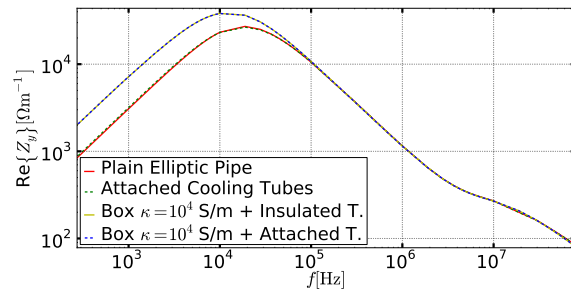


Figure 8: Vert. imp. of proposed SIS100 pipe setups

ferent setups occur only at extremely low frequencies, i.e. below the range reachable by the specified betatron tunes.

For the longitudinal impedance the numerical method has to be restricted to the frequency range for which radial and axial model coincide. The revolution frequency of SIS100 provides the validity of the method to calculate the beam induced heat load. The calculated beam induced heat load is negligibly small compared to the heat load during the magnet ramp.

The transverse impedance in the relevant frequency range cannot be reduced since this needs a change of the pipe itself. The applicability of a feedback system will be discussed in future.

REFERENCES

- [1] R. Gluckstern, *Analytic Methods for Calculating Coupling Impedances*, Cern Accelerator School, 2000.
- [2] H. Hahn, *Matrix solution for the wall impedance of infinitely long multilayer circular beam tubes*, Phys. Rev. ST Accel. Beams, 2010.
- [3] G. Nassibian and F. Sacherer, *Methods for measuring transverse coupling impedances in circular accelerators* Nucl. Instrum. Meth., 1979.
- [4] L. Vos, *The Transverse Impedance Of A Cylindrical Pipe With Arbitrary Surface Impedance*, IEEE JMTT, 2003.
- [5] T. Kroyer, *Simulation of the low frequency Collimator Impedance*, CERN-AB-2008-017
- [6] CST Studio Suite 2010®, www.cst.com
- [7] S. Wolfram *Mathematica 7.0*®, www.wolfram.com, 2010